www.icgst.com

Fast Segmented Reconstruction Technique for Magnetic Resonance Imaging under B0 Inhomogeneity

Yasser M. Kadah
Biomedical Engineering Department, Cairo University, Giza, Egypt,
E-mail: ymk@k-space.org,
http://ymk.k-space.org

Abstract
The conjugate phase method is a general effective reconstruction method for magnetic resonance imaging under B0 inhomogeneity. This method, when implemented in its exact form, is associated with a rather heavy computational burden. In this work, we describe a new implementation of this method that reduces substantially the computational complexity of the conjugate phase method based on field map discretization and use of gridded data. In this method, the field map is segmented into a number of levels and the raw k-space is gridded. Then, the conjugate phase method is used to compute the correction for each field level instead of each point using the gridded k-space. The results of correcting all levels are subsequently added to obtain the corrected image. The new method is demonstrated by applying it to correct experimental result from a spiral imaging sequence.

Keywords : *Magnetic resonance imaging, B0 field inhomogeneity, artifact suppression, image reconstruction.*

1. Introduction
In magnetic resonance imaging, spatial localization is achieved by applying linear magnetic field gradients that induce a linear relationship between each location and its resonance frequency according to Larmor equation. When the static magnetic field B0 is not homogeneous, the resultant mapping becomes distorted. Such distortion is more problematic in cases when fast acquisition involving long echo readout is used. In this case, several forms of artifacts may appear in the resultant images depending on the way the k-space is traversed. For example, when the k-space trajectory is linear such as echo-planar imaging (EPI), the distortion appears in the form of spatially variant pixel shifts. On the other hand, when the k-space trajectory is spiral, the distortion causes spatially varying blur in the resultant images. Other trajectories such as segmented EPI with centric reordering may contain both shift and blur. Such distortions are not simple to correct for and usually a heavy computational cost is involved in the process of removing such geometric distortion. This is particularly of concern to such methodologies as functional magnetic resonance imaging (fMRI) where a large number of images are acquired and need to be corrected. With several real-time implementations of fMRI analyses already available in commercial magnetic resonance scanners, the complexity of the correction algorithms is of particular importance given the real-time requirements of this technology.

Several techniques have been proposed to correct for this distortion. All these techniques rely on a B0 field mapping methodology based on acquiring two images with slight difference in echo time. Such field map is used to estimate and reverse the distortion in the reconstructed image. The simplest yet the most limited is the technique proposed by Jizzard and Balaban [1] where the pixel shifts due to B0 inhomogeneity in linear k-space trajectories are computed and interpolation is used to compute the correct image after removing these shifts. Since this technique does not consider the removal of blur, it is not suitable for k-space trajectories that are not linear in nature. Alternatively, the conjugate phase method introduced by Maeda et al. [2] and its variants [3-5] reconstructs images with reduced distortion from the k-space data based on *a priori* knowledge of the magnetic field in the slice of interest. This technique offered generality to all k-space trajectories including spiral imaging. Another technique that offers the same generality is the simulated phase evolution rewinding (SPHERE) method proposed by Kadah and Hu [6] which appears to provide better correction while relying on fast imaging based field mapping. Discretization of the reconstruction inverse problem was also proposed in [7] where the reconstruction takes the form of a solution to linear system of equations. A comparison between available techniques was done in [8] and several practical implementation methods were introduced for all methods. The results of this work suggested that some of the variants of the conjugate phase methods provide better results and lower computational complexity. Unfortunately, the computational complexity of any of these implementations is still too high for such applications as real-time fMRI and therefore a further reduction of the computational cost is still desired. Given that the conjugate phase methods and its variants are the most widely used correction methods for complex k-space trajectories, it is desired to have a methodology that allows this chosen technique to have a lower complexity.

Another motivation for this work is the current interest in iterative sparse image reconstruction techniques where a huge linear system of equations with sparse matrix components is solved to reconstruct the image [9-10]. Compressed sensing theory has been also used to provide stable solutions to such systems in the case when several undersampling is involved [11-12]. In both approaches, adding the B0 inhomogeneity correction to the problem is possible but significantly delays the convergence of these methods thus adding a prohibitively large cost in computational complexity. Given that the above B0 inhomogeneity correction methods rely on correcting the raw data during the reconstruction process, it is desirable to separate the reconstruction and correction processes to enable the correction to be done after the reconstruction is finished. This allows the new reconstruction methods to be performed first without any new constraints to maintain their computational efficiency then the B0 correction is done on the gridded k-space of the reconstruction.

In this paper, a new segmented implementation of the conjugate phase method is described based on field map discretization and using the k-space data after gridding. In this method, the field map is discretized into a number of levels. A spatial domain mask corresponding to all locations with similar field level is created for all possible levels. The conjugate phase method is used to compute the reconstruction for all points with the same field level simultaneously. The results of different levels are subsequently added to create the final image. Since the gridded k-space data are used as the input to the reconstruction procedure, the reconstruction at each level is a low complexity 2D Fourier transformation. The new method maintains a more exact k-space correction besides allowing the use of high complexity gridding or sparse sampling procedures. The implementation details of the new approach are described and the performance is demonstrated by experimental results.

The remainder of the paper is organized as follows: Section (2) presents the theory and description of the methodology, Section (3) presents the experimental verification, Section (4) presents a discussion of the results and finally Section (5) summarizes the conclusions of this work.

2. Theory

The conjugate phase method takes the following mathematical form,

$$\hat{f}(\vec{r}) = \int_{-\infty}^{\infty} F(\vec{k}) \cdot e^{-j2\pi\gamma\Delta B(\vec{r})t(\vec{k})} d\vec{k} \quad , \qquad (1)$$

where $\hat{f}(\vec{r})$ is the corrected image , $F(\vec{k})$ is the available k-space values, γ is the gyromagnetic ratio, $\Delta B(\vec{r})$ is the field inhomogeneity, and $t(\vec{k})$ is the sampling time of k-space points. The main advantage of this method is its generality for use with any k-space traversal trajectory. Unfortunately, with complex trajectories such as with spiral imaging, the computational complexity of this method may become rather high ($\boldsymbol{O}(N^4)$ flops/image). This complexity is prohibitive for practical imaging conditions especially when the matrix size is of the order of 128 or larger.

A reduced-complexity modification of the conjugate phase method was proposed in [8] where the obtained k-space, or equivalently $t(\vec{k})$ is divided into a number of segments each considered as an instant in the correction. This technique provides flexible control over the complexity/accuracy trade-off encountered with the conjugate phase method. The complexity of this technique reaches the limit of the exact conjugate phase method when the number of segments approaches the number of k-space points. When the number of segments is chosen as a smaller value, there will be a reduction in the complexity of the technique accompanied by some loss of accuracy. In spite of the satisfactory results obtained with this technique, the assumptions used in this technique put some limits on the attainable reconstruction accuracy at reasonable computational complexities. For example, the results in [8] were based on a short imaging window length of 2 ms. In practice, the imaging window is usually longer and in some cases it is nearly two orders of magnitude longer as with echo-planar imaging and single-shot spiral imaging sequences. In this case, the number of segments required for an accurate reconstruction may not be small and the complexity of this technique becomes high. Furthermore, this technique uses a low complexity gridding algorithm that is based on bilinear interpolation. As a result, more elaborate gridding procedures cannot be used with this technique resulting in suboptimal point spread function. Therefore, a reduced complexity technique that does not rely on these limiting assumptions would have a clear advantage.

As with the original conjugate phase method, a field map is required for the slice of interest in order to perform the correction. To reduce additive noise contamination in the field map, it is first smoothed using a spatial low-pass filter of a width of 5 pixels. The range of values this field map contains is discretized into L levels such that,

$$\Delta\hat{B}(\vec{r}) = \text{INTEGER}\left((L-1) \cdot \frac{\Delta B(\vec{r}) - \min\{\Delta B(\vec{r})\}}{\max\{\Delta B(\vec{r})\} - \min\{\Delta B(\vec{r})\}} \right). \qquad (2)$$

Here, $\Delta\hat{B}(\vec{r})$ is an integer array containing the discrete version of the original field map $\Delta B(\vec{r})$, $\min\{\Delta B(\vec{r})\}$ is the minimum field value, and $\max\{\Delta B(\vec{r})\}$ is the maximum value. Using the discrete field map, spatial domain masks are generated by simply including all points with a given field level. That is, each mask corresponds to all points in the image that have the same inhomogeneity level. In a mathematical form,

$$M_l(\vec{r}) = \begin{cases} 1 & , \quad \Delta\hat{B}(\vec{r}) = l \\ 0 & , \quad otherwise \end{cases} \quad , \qquad (3)$$

where $M_l(\vec{r})$ is the mask for field level l and sums up to 1 within the field of view for all values of l.

Subsequently, instead of using Eq.(1) to compute each point in the image separately, it is modified to obtain all points in the image having the same inhomogeneity level. In this case, the corrected image $\tilde{f}(\vec{r})$ takes the form,

$$\tilde{f}(\vec{r}) = \sum_{l=0}^{L-1} M_l(\vec{r}) \cdot \int_{-\infty}^{\infty} F(\vec{k}) \cdot e^{-j2\pi\gamma\Delta\hat{B}_l t(\vec{k})} \cdot e^{j2\pi\vec{k}\cdot\vec{r}} d\vec{k} \quad , (4)$$

with,

$$\Delta\hat{B}_l = l \cdot \left(\max\{\Delta B(\vec{r})\} - \min\{\Delta B(\vec{r})\}\right) / L + \min\{\Delta B(\vec{r})\} . \ (5)$$

An illustration of the field map discretization and the generation of spatial masks is shown in Figure 1.

The exact implementation of the conjugate phase method requires a computationally expensive gridding procedure to be repeated for each of the L reconstruction steps. Although the new method would still be much faster than the original using the exact implementation, further reduction in the computational complexity is still desirable for practicality. Therefore, an approximate implementation is developed where the gridding procedure is applied once and the gridded k-space is used as the input to the correction procedure. Given that each point in the gridded k-space is composed of many contributions from different spiral samples, the following procedure is used to estimate the approximate value of the time variable at each point in the k-space. A timing array of the same size as the array of spiral sample is created and each element is assigned an integer value based on the sampling time of the corresponding element in the spiral data array. For example, when a segmented spiral sequence is used to acquire 16 segments, each containing 1024 points, the timing array will be composed of 16×1024 array with 16 identical rows each containing the values from 0 to 1023. Then, this array is used as the input to the gridding program. The outcome of this gridding procedure is subsequently considered as an estimate of $t(\vec{k})$ of the gridded k-space needed in the correction procedure. As a result, the reconstruction complexity when these gridded data are used will be similar to a 2D FFT operation, which is relatively inexpensive. An illustration of the process of generating $t(\vec{k})$ is shown in Figure 2 for a sequence with S segments. A practical illustration of the result for its computation is illustrated in Figure 3 for a spiral imaging sequence where the center of the k-space acquisition starts in the center of the image and moves outside radially. Therefore, the center of the image has the smallest sampling time while the outside of acquired area has the largest time.

3. Experimental Results

The new method was used to correct experimental data of different resolution phantom and normal human volunteers obtained from a 1.5T Siemens Magnetom Vision MR scanner (Erlangen, Germany). The magnetic field used in all cases was not properly shimmed to allow magnetic field inhomogeneity to be more apparent. The imaging sequence used was a spiral sequence with 16 segments, each taking 10.24 ms. The imaging parameters were: TR/TE: 1000/6 ms, FOV: 31 cm × 31 cm, matrix size 128×128. The field maps were obtained using a FLASH sequence using two images with a 3 ms difference in echo times. The field map estimate is obtained from the phase difference between the two images scaled by the echo time difference. The field maps are masked to null the field map in background areas outside the imaged object and smoothed using a square kernel of 7 pixels wide to reduce noise. The spiral data were gridded using a Kaiser-Bessel window of width 7 pixels according to [13]. A block diagram of the procedure is shown in Figure 4 and an illustration of the different reconstructions for different numbers of levels is shown in Figure 5.

The reconstruction results are illustrated in Figures 6 for resolution phantoms and 7 for human volunteers for different numbers of levels L. The B0 inhomogeneity distortion manifests itself as severe blurring, pixel shift and occasional signal loss in severe cases. The field map estimated for each case is shown to the right and a reference undistorted image acquired using the slower FLASH sequence is shown in the second column. The columns from 3 to 8 illustrate the results for each phantom with numbers of levels 4, 8, 16, 32, and 128 respectively. As can be observed, the correction accuracy improves gradually with the number of field levels. Also, efficient correction can be obtained at values of L as low as 8, which makes the reconstruction procedure quite fast. It should be noted that the reconstruction time depends linearly on the number of levels. That is, the reconstruction time of level 16 for example takes half that for 32 levels and a quarter of that for 128 levels. Given that in the original conjugate phase reconstruction the number of levels is much higher than that, the computational complexity advantage is evident in the new method.

Given the fact that field map discretization causes field map errors, it is desired to analyze such errors versus the number of levels to ensure that they are not excessive. In Figures 8 (phantom data) and 9 (human data), the percentage error is shown with error bars representing the standard deviation of this error. As can be observed, the error becomes within the known field map estimation error range of 5% after 32 levels. In Figure 10, the percentage root-mean-square error in image reconstruction is shown verses the number of levels used for both phantom and human experiments. The error was computed based on the difference between the reconstruction using the new method and the one provided by the original conjugate phase method. This figure suggests the minimal impact on the image quality beyond 32 levels.

4. Discussion

The basic assumption of the new method is that the discretization of the field map does not have a significant effect on the correction procedure. In order to verify this assumption, the percentage maximum deviation of the discrete field map from the original was computed for different field maps. As it turned out, the deviation is only a few percent for numbers of levels as low as 16. In order to compare this deviation to the statistical variation of field mapping values from the usual contamination by noise, a number of independent field maps were obtained for the same slice and the variation of individual maps from their average as an estimate for the exact map was computed. The obtained variations were found to be in the same range of a few percent as what is encountered with discretization. Moreover, the use of one of these field maps or another with the conjugate phase method did not make any difference even though when they are slightly different. This suggests that the conjugate phase method is robust to such variations and that making use of this property by the present method is justified.

It should be emphasized that the uniform discretization of the range of values of the field map is rather arbitrary. Several strategies can be proposed to use nonuniform discretization in order to optimize the accuracy of the technique. For example, when one of the uniform levels contains a small number of points, it might be computationally advantageous to merge it with a neighboring level without affecting the accuracy of the reconstruction by much. On the other hand, when one level contains a very large number of points, it is advantageous to divide it into sublevels to allow for more accurate reconstruction. These approaches are therefore problem dependent and should be designed based on the data at hand.

The computational complexity of this technique is dominated by the 2D FFT procedures used in each of the L steps to obtain the images. Therefore, to reconstruct an $N \times N$ image using L steps of the new method, the estimated complexity is $O(L\ N^2 \log N)$ flops/image. For the commonly used large values of images and image size N, the new method amounts to several orders of magnitude reduction in the number of required computations. In fact, for a matrix size of 128 and a number of field levels of 16, the new method takes only a few tens of milliseconds on modern personal computers to compute the correction, which is considered practical in current MR protocols (e.g., functional MRI). The current approach lends itself to parallel implementation taking advantage of modern dual and quad core processors where the reconstruction for each level is an independent process that can run in parallel with other similar processes from other levels. Moreover, for such applications as fMRI where the same slice is acquired a large number of times, the burden of computing the masks is done only once given that the field map for the same slice does not change with time. This suggests the potential for this technique for real-time fMRI applications.

It should also be noted that applying the correction with a certain number of levels does not preclude the possibility of further improvement later on. That is, one can use a number of levels of 16 to meet the requirements of a real-time application and then reconstruct an improved version of the same image sequence using 128 levels for further off-line analysis if desired. In this case, the field map is taken to be the difference between the discretized maps for these levels. This progressive reconstruction capability allows flexibility to the user based on the clinical application at hand.

5. Conclusions

A fast implementation of the conjugate phase correction was developed. The technique uses an L-level discretization of the field map to create L groups of points with similar field values. These groups are subsequently corrected together, significantly reducing the computational complexity of the correction procedure. Also, instead of repeating the gridding procedure in each of these L reconstruction steps, the gridding process is performed only once and the gridded data are used as the input to the reconstruction procedure to further reduce the complexity of the technique. The new method is demonstrated to be effective by experimental results. The new approach can be useful in such applications as real-time functional magnetic resonance imaging where many images need to be corrected for field inhomogeneity.

6. References

[1] P. Jezzard and R. S. Balaban, “Correction for geometric distortion in echo planar images from Bo field variations,” *Magnetic Resonance in Medicine*, vol. 34, pp. 65–73, 1995.

[2] A. Maeda, K. Sano. and T. Yokoyama, “Reconstruction by weighted correlation for MRI with time-varying gradients,” *IEEE Transactions on Medical Imaging*, vol. 7, no. 1, pp. 26-31, 1988.

[3] D.G. Noll, C.H. Meyer, J.M. Pauly, D.G. Nishimura, and A. Macovski, “A homogeneity correction method for magnetic resonance imaging with time-varying gradients,” *IEEE Transactions on Medical Imaging*, vol. 10, no. 4, pp. 629-637, 1991.

[4] D.C. Noll, J.A. Fessler, B.P. Sutton, “Conjugate phase MRI reconstruction with spatially variant sample density correction,” *IEEE Transactions on Medical Imaging*, vol. 24, no. 3, pp. 325-336, March 2005,

[5] B.P. Sutton, D.C. Noll, J.A. Fessler, “Fast, iterative image reconstruction for MRI in the presence of field inhomogeneities,” *IEEE Transactions on Medical Imaging*, vol. 22, no. 2, pp. 178-188, 2003.

[6] Y.M. Kadah and X. Hu, “Simulated phase evolution rewinding (SPHERE): a technique for reducing B0 inhomogeneity distortion in MRI,” *Magnetic Resonance in Medicine*, vol. 38, pp. 615-627, 1997.

[7] Y.M. Kadah and X. Hu, “Algebraic reconstruction for magnetic resonance imaging under B0 inhomogeneity,” *IEEE Transactions on Medical Imaging*, vol. 17, no.3, pp. 362-70, 1998.

[8] H. Schomberg, “Off-resonance correction of MR images,” *IEEE Transactions on Medical Imaging*, vol. 18, no. 6, pp. 481-495, 1999.

[9] Y.M. Kadah, A. Fahmy, R. Gabr, K. Heberlein, and X. Hu, “Progressive magnetic resonance image reconstruction based on iterative solution of a sparse linear system,” *International Journal of Biomedical Imaging*, vol. 2006, pp. 1-9, 2006.

[10] R.E. Gabr, P. Aksit, P.A. Bottomley, A.M. Youssef, and Y.M. Kadah, “Deconvolution-interpolation gridding (DING): accurate reconstruction for arbitrary k-space trajectories,” *Magnetic Resonance in Medicine*, vol. 56, pp. 1182-1191, December 2006.

[11] M. Lustig, D.L. Donoho, J.M. Pauly, "Sparse MRI: the application of compressed sensing for rapid MR imaging," *Magnetic Resonance in Medicine*, vol. 58, pp. 1182-1195, 2007.

[12] U. Gamper, P. Boesiger, S. Kozerke, "Compressed sensing in dynamic MRI," *Magnetic Resonance in Medicine*, vol. 59, pp. 365-373, 2008.

[13] J.I. Jackson, C.H. Meyer, D.G. Nishimura, and A. Macovski, "Selection of a convolution function for Fourier inversion using gridding," *IEEE Transactions on Medical Imaging*, vol. 10, no. 3, pp. 473-478, 1991.

7. Biography

Dr. Yasser M. Kadah received his B.Sc. and M.Sc. degrees from the Biomedical Engineering Department at Cairo University in 1989 and 1992 respectively. He received his Ph.D. in Biomedical Engineering from the University of Minnesota in 1997. He worked as a research assistant with the Department of Radiology, University of Minnesota Medical School in 1996-1997 and as a post-doctoral fellow at the Center of Magnetic Resonance Research at the University of Minnesota in 1998. He became an Assistant Professor of Biomedical Engineering at Cairo University from 1998 to 2003. He also worked during the same period as the director of research and development at IBE technologies, Egypt. He also was a Research Associate with the Biomedical Imaging Technology Center at the Biomedical Engineering Department, Emory University and Georgia Institute of Technology, from December 2002 till July 2004. He is currently an Associate Professor of Biomedical Engineering at Cairo University. Along his career, he received several awards and recognitions including the record for highest undergraduate GPA in the department of Biomedical Engineering at Cairo University, the IDB Merit Scholarship (1993-1996), his biography was selected to appear in Marquis Who's Who in the World in 2002, as well as winning the E.K. Zaviosky stipend from the international society of magnetic resonance in imaging in 2002. He was also elected a Senior Member of the Institute of Electrical and Electronic Engineers (IEEE) in 2003. He received the State Encouragement Award in Engineering Sciences from the Academy of Scientific Research and Technology, Egypt in 2006. He was also selected to receive an award from the Cairo University Faculty Club as the 2007 professor of the year in biomedical engineering. He was the Scientific Program Chair for the Third Cairo International Biomedical Engineering Conference (CIBEC'06), which was held in Cairo in December 2006. He is currently an active member of the International Society of Magnetic Resonance in Medicine (ISMRM) and the International Society of Optical Engineering (SPIE). His research interests include medical imaging and in particular MRI and ultrasound, and multi-dimensional signal processing for biomedical applications.

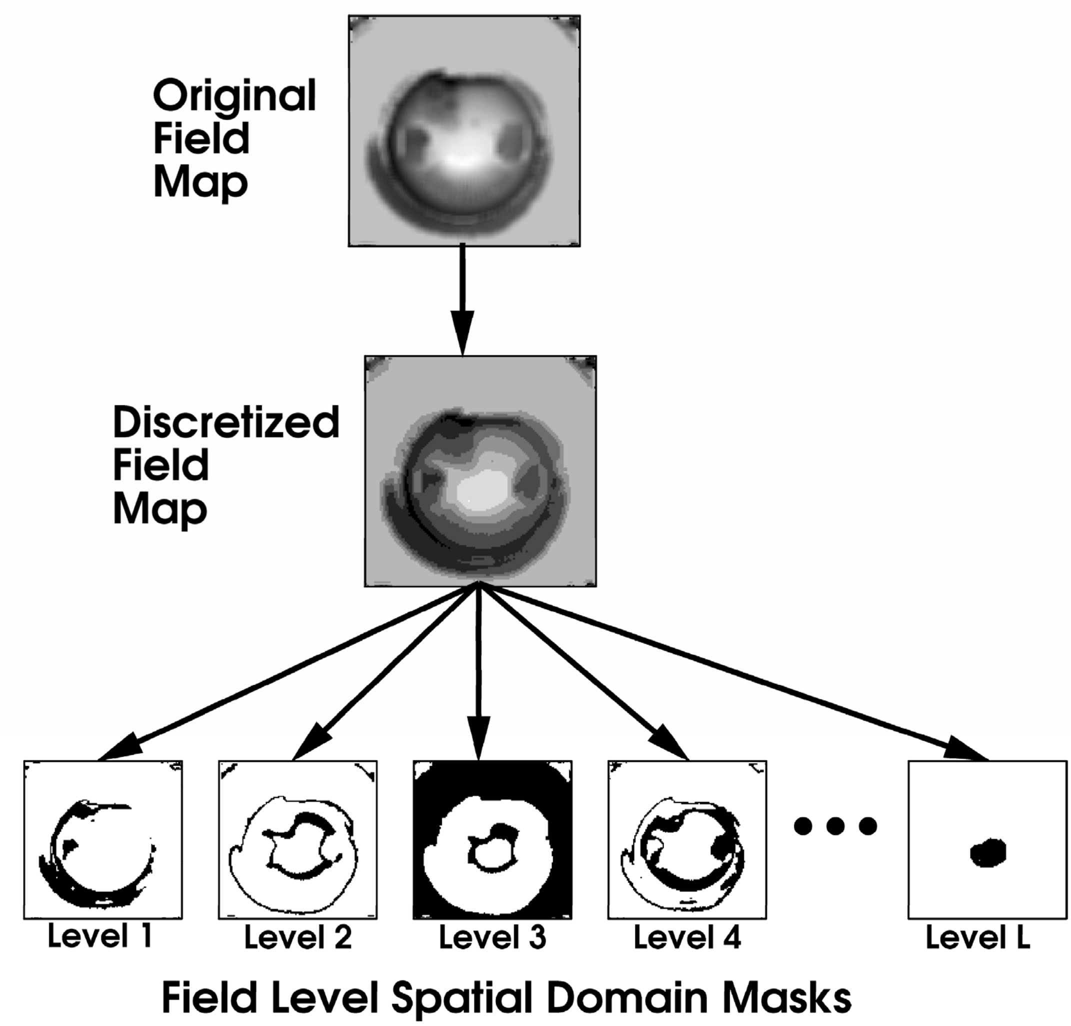

Figure 1: Illustration of field map discretization and the generation of spatial domain mask.

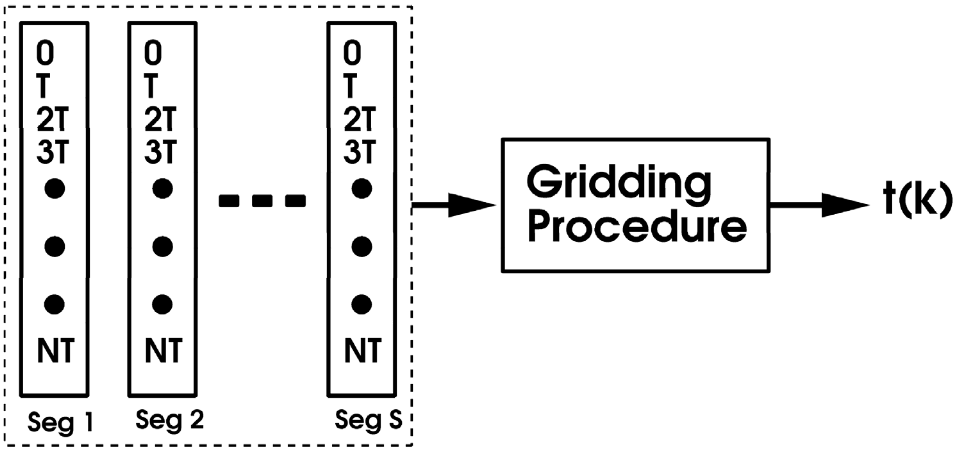

Figure 2: Illustration of the procedure used to generate the timing function by gridding.

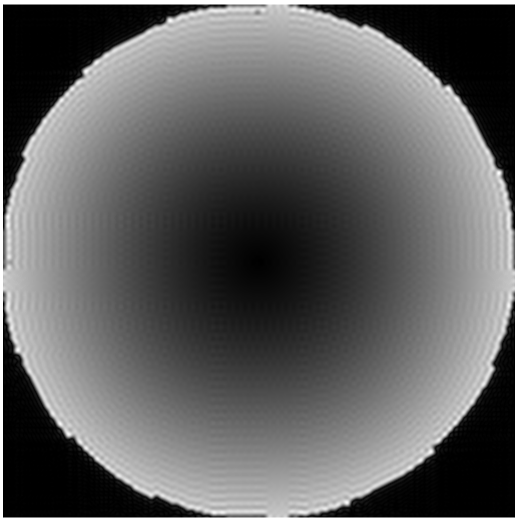

Figure 3: Illustration of the timing function obtained by gridding for spiral trajectory.

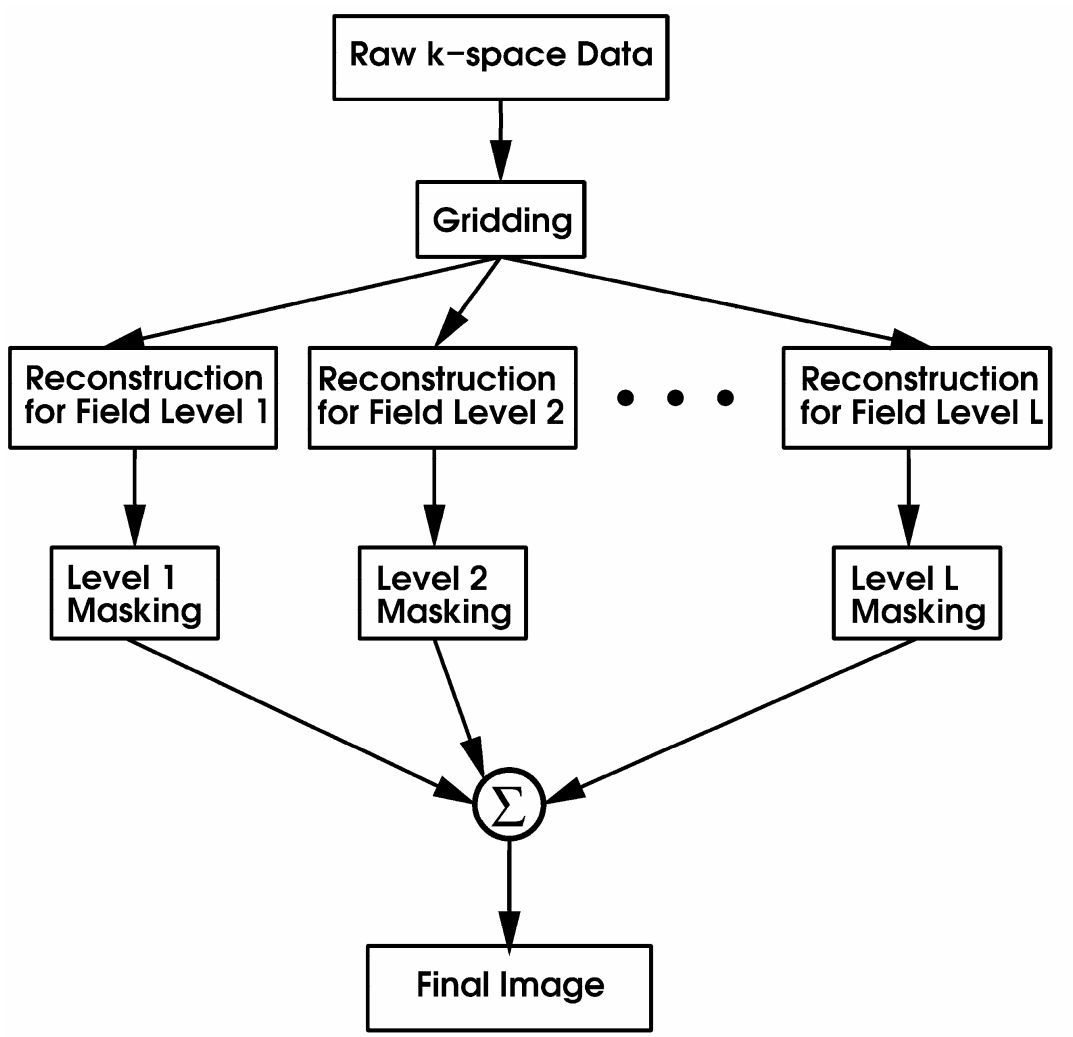

Figure 4: Block diagram of the segmented correction method.

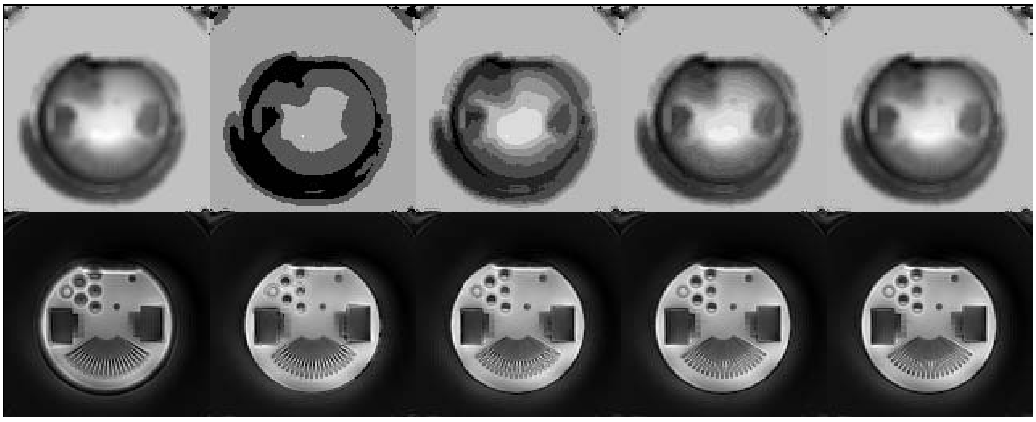

Figure 5: Illustration of segmented correction for different numbers of levels. At the left column, the original field map and the distorted object. The following columns represent the discretized field maps and the corrected objects for 4, 8, 16, and 32 field levels respectively.

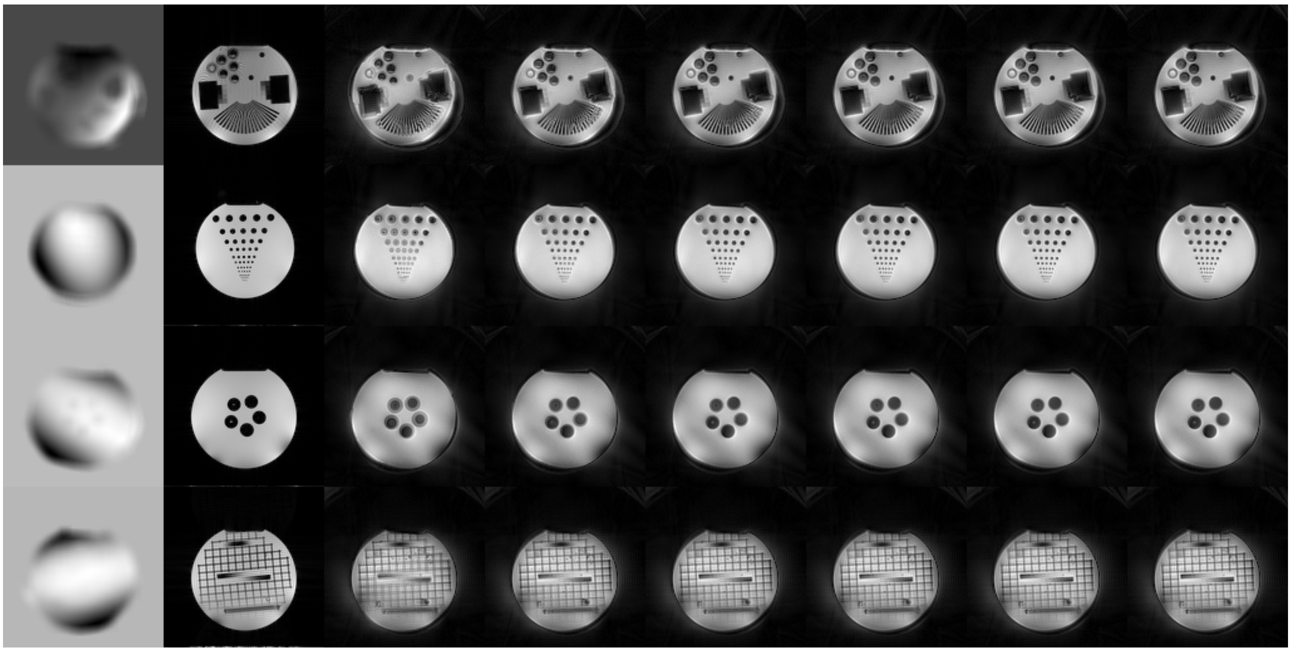

Figure 6: Results of segmented correction of resolution phantom images for different numbers of levels. At the left column, the original field map is shown, and the second column show a reference image obtained using FLASH sequence. The columns 3-8 show the correction results for 4, 8, 16, 32, 64 and 128 field levels respectively.

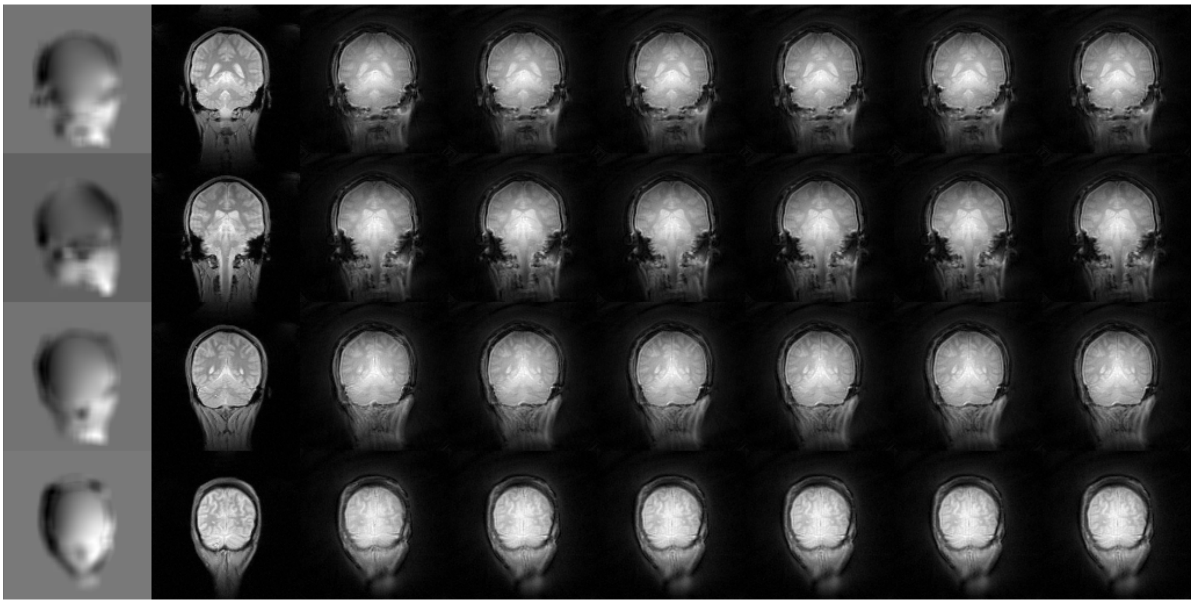

Figure 7: Results of segmented correction of human volunteer images for different numbers of levels. At the left column, the original field map is shown, and the second column show a reference image obtained using FLASH sequence. The columns 3-8 show the correction results for 4, 8, 16, 32, 64 and 128 field levels respectively.

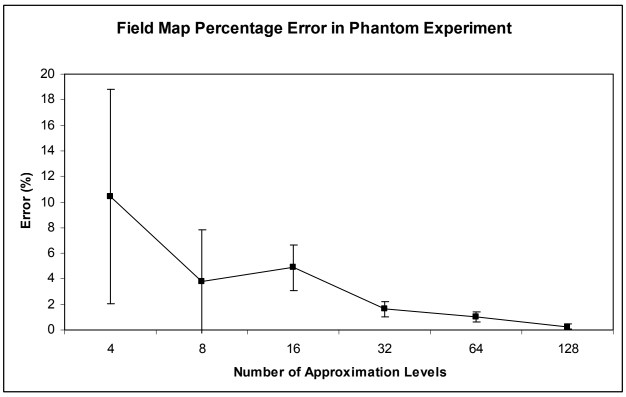

Figure 8: Illustration of the relative error in field maps versus the number of field map approximation levels in resolution phantoms.

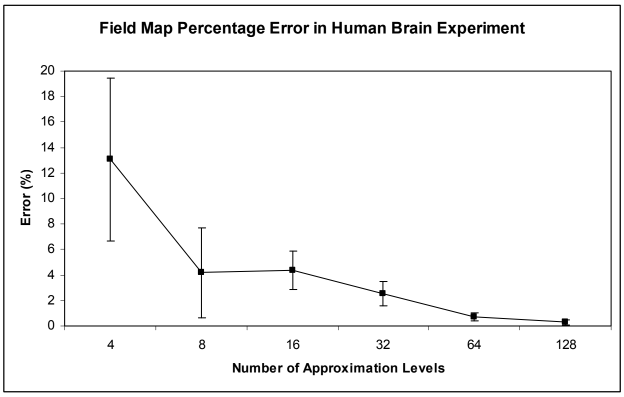

Figure 9: Illustration of the relative error in field maps versus the number of field map approximation levels in human volunteers.

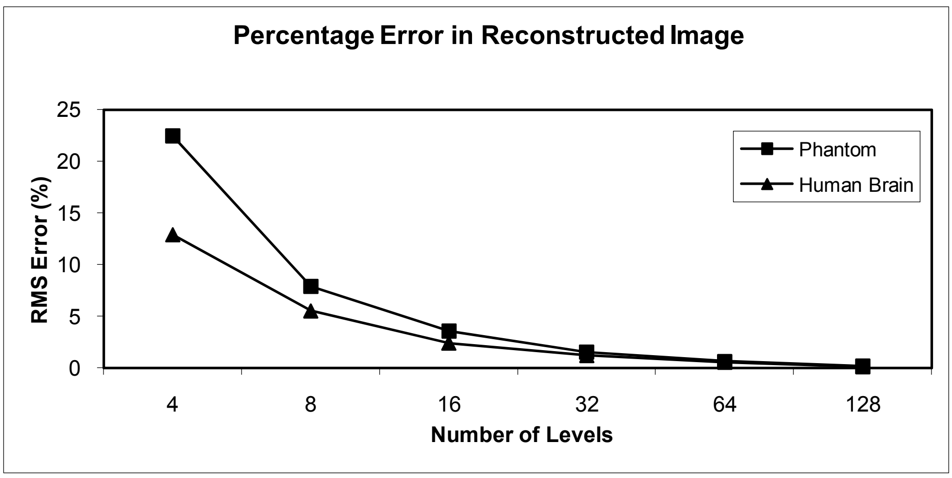

Figure 10: Illustration of the RMS error in image reconstruction versus the number of field map approximation levels in both resolution phantoms and human volunteers.